

Original article

Optimizing corrosion resistance of anodized TiO₂ coatings through controlled calcination parameters

Optimización de la resistencia a la corrosión de recubrimientos de TiO₂ anodizados mediante parámetros controlados de calcinación

William Alexander Aperador-Chaparro¹, José Barba-Ortega², Miryam Rincón-Joya^{2,*}

¹ Universidad Militar Nueva Granada, Bogotá, Colombia

² Grupo de Física mesoscópica, Departamento de Física, Universidad Nacional de Colombia, Bogotá D.C., Colombia

Abstract

We studied how calcination parameters such as temperature and duration influence the phase composition and corrosion resistance of anodized titanium dioxide (TiO₂) coatings. We synthesized TiO₂ anatase and rutile phases on titanium surfaces via anodization at 40 V followed by calcination at 350°C and 450°C, respectively. We used electrochemical impedance spectroscopy (EIS) to assess these properties and behaviors. Our results indicated that longer calcination times and higher temperatures favored the rutile phase and shorter times resulted in coatings with a mixture of anatase and rutile. The rutile phase exhibited superior corrosion resistance due to its more complete crystallization and reduced structural defects. These results underscore the importance of optimizing calcination parameters to achieve desired crystalline phases and enhance corrosion resistance, with promising implications for applications in corrosive and mechanically challenging environments.

Keywords: Rutile; Anatase; Anodizing; Electrochemical impedance spectroscopy (EIS).

Resumen

Estudiamos aquí cómo parámetros de calcinación como la temperatura y la duración influyen en la composición de fases y la resistencia a la corrosión de los recubrimientos de dióxido de titanio (TiO₂) anodizados. Se sintetizaron las fases de anatasa y rutilo del TiO₂ en superficies de titanio mediante anodización a 40 V, seguida de calcinación a 350 °C y 450 °C, respectivamente. Se utilizó la espectroscopía de impedancia electroquímica (EIS) para evaluar estas propiedades y comportamientos. Los resultados indicaron que los tiempos de calcinación más largos y las temperaturas más altas favorecieron la fase rutilo, en tanto que los tiempos más cortos resultaron en recubrimientos con una mezcla de anatasa y rutilo. La fase rutilo mostró una resistencia superior a la corrosión debido a una cristalización más completa y la reducción de defectos estructurales. El estudio subraya la importancia de optimizar los parámetros de calcinación para alcanzar las fases cristalinas deseadas y mejorar propiedades como la resistencia a la corrosión, con implicaciones prometedoras para aplicaciones en entornos corrosivos y sujetos a desgaste mecánico.

Palabras clave: Rutilo; Anatasa; Anodización; Espectroscopía de impedancia electroquímica (EIS).

Introduction

Due to their versatility and wide range of applications in modern science and technology, nanostructured materials, especially TiO₂, are crucial research topics (Mansfeldova, 2021; Manut, 2020). Their use in various commercial products, from cosmetics to solar cells, highlights their importance across multiple fields. Nanocrystalline TiO₂ synthesis focuses on its role as a photocatalyst (Lin, 2014; Seul, 2022) in environmental applications such as hydrogen production using solar energy. Titanium dioxide (TiO₂) is widely used for

Citation: Aperador Chaparro WA, *et al.* Optimizing corrosion resistance of anodized TiO₂ coatings through controlled calcination parameters. Revista de la Academia Colombiana de Ciencias Exactas, Físicas y Naturales. 48(188):483-490, julio-septiembre de 2024. doi: <https://doi.org/10.18257/racefyn.2652>

Editor: Rafael González Hernández

***Corresponding autor:**

Miryam Rincón Joya;
mrinconj@unal.edu.co

Received: May 24, 2024

Accepted: July 31, 2024

Published on line: August 30, 2024



This is an open access article distributed under the terms of the Creative Commons Attribution License.

energy conversion and storage, sensors, cosmetics, paints, and electronics. TiO₂ exists naturally in several polymorphic forms (Seul, 2022), the most common being rutile, brookite, and anatase. Anatase TiO₂ stands out for its superior charge separation and ion storage capabilities compared to other polymorphs. This is useful in nanocrystalline solar cells, photocatalysis, and lithium-ion batteries (Baram, 2010; Li, 2019). However, thermodynamically, rutile TiO₂ is the most stable polymorphic form under ambient conditions (Seul, 2022; Quitério, 2015).

Catalysts utilizing TiO₂ continue to find widespread use in photocatalysis and H₂ production through water photoelectrolysis (Sanoja, 2024). The anodic oxidation technique of titanium sheets has become increasingly popular for fabricating TiO₂ films with a nanostructured morphology. Research has aimed to enhance the performance of these materials as photoanodes in visible light-driven H₂ generation, exploring heterojunction formation or cocatalyst incorporation to tune their catalytic activity (Pasquale, 2023; Parambil, 2023). In the quest for efficient photocatalysts, the importance of an organized three-dimensional arrangement of TiO₂ nanotubes on a mesh stands out, leveraging their extensive internal and external surface areas. This facilitates light absorption from various directions resulting in enhanced efficacy in water photoelectrolysis. Studies have demonstrated that nanotubes grown on titanium wires can effectively capture light reducing liquid scattering effects and improving photocatalytic activity (Pasquale, 2023).

Erosion-corrosion, a phenomenon characterized by the rapid degradation of metals due to chemical interactions and mechanical wear from fluid-solid particle motion, is prevalent in corrosive industrial settings (Thakur, 2024; Sarngan, 2022). Conversely, anodizing is an electrochemical technique that enhances the surface properties of materials like titanium, forming a protective oxide layer that boosts corrosion resistance and other desirable traits. While erosion-corrosion results from combined chemical and mechanical factors, anodizing is a controlled method to create a protective oxide layer. Here, we initially employed the anodizing process (Suhadolnik, 2020; Gabellini, 2023). However, recent research underscores challenges in reproducibility within the titanium anodization process, particularly in fluoride solutions, highlighting the need for further exploration of electrolyte compositions to consistently produce high-quality TiO₂ films unaffected by electrolyte aging (Arzaee, 2023; Yu, 2023). Titanium dioxide (TiO₂) is a widely used material in several fields, its most common forms being rutile, brookite, and anatase. Anatase TiO₂ stands out for its ability to separate charges and ion storage properties, making it ideal for nanocrystalline solar cells, photocatalysis, and lithium-ion batteries (Kim, 2022; Ali, 2018; Eddy, 2023). However, rutile TiO₂ is the most thermodynamically stable polymorphic form under ambient conditions for which there is interest in its large-scale and cost-effective production (Kim, 2022).

The difference in surface energy between the rutile and anatase forms plays a crucial role in their stability, especially in smaller particles. Although in its rutile form, TiO₂ is more stable, wet methods often produce anatase due to its lower surface energy. Here we transformed rutile particles to anatase through an anodization process resulting in the rutile phase and a mixture of anatase and rutile phases. Our main objective was to study the behavior of anodized TiO₂ through electrochemical EIS studies and discuss its crystalline properties and response to corrosion.

Materials and methods

The electrochemical anodization of 2 cm² Ti foils (99.99% high purity and 0.12 mm thick) was done in a homemade setup as previously detailed (Mateus, 2019; Bautista, 2018), at room temperature using a 50 V power supply. The electrolyte consisted of an ethylene glycol solution containing NH₄F (0.2% by weight) and H₂O (2% by weight). All samples were subjected to a potential of 40 V for 30 minutes (Mateus, 2019; Bautista, 2018).

Sample 1 was anodized at 40 V and subsequently calcined at 350 °C for five hours. Sample 2 underwent anodization at 40 V and a two-hour calcination at 350 °C. Sample

3 was anodized at 40 V and calcined at 450 °C for two hours. Each sample was then sequentially rinsed with ethanol and deionized water. To obtain the X-ray diffraction (XRD) patterns of the anodized Ti foil, a Panalytical Empyrean device was used in a continuous beam configuration with a scintillation detector and a parallel plate collimator. Measurements were taken from 10 to 90° at a 2θ angle with a sampling time of 0.02 seconds and a step size of 0.0040°/s using cobalt radiation with a wavelength of $K\alpha_1 = 1.78900 \text{ \AA}$. The atomic force microscopy images were obtained on a Bruker Dimension Technology KIT equipment. The electrochemical study was conducted using a potentiostat (Gamry PCI4300) equipped with Gamry framework (version 4.21/EIS 300 software), employing electrochemical impedance spectroscopy (EIS). The impedance curves were obtained at room temperature using a cell housing a working electrode within an exposed area (1 cm²), a reference electrode (Ag/AgCl), and a graphite counter electrode in a 0.5 M NaCl solution with distilled water. The open-circuit potential was measured for 30 minutes (Aperador, 2012). We analyzed the electrochemical behavior of the electrolyte via EIS at open-circuit potential for 30 minutes to establish its stable values that served as the starting point for the EIS measurements.

Results and discussion

The TiO₂ crystalline structure of titanium dioxide is of great interest for its multiple polymorphic forms, prominently rutile and anatase. Rutile exhibits a tetragonal crystalline structure, offering superior stability at elevated temperatures and a high density. Its applications span from white pigments to optical coatings and high-temperature applications owing to its stability. Conversely, anatase showcases a tetragonal crystalline structure akin to rutile but with a slightly different atomic arrangement. Its properties render it more active than rutile in photocatalytic reactions, attributed to its energy band structure making it an optimal choice for photocatalysis, solar cells, self-cleaning coatings, and biomedical applications, leveraging its photocatalytic properties.

Figure 1a shows sample 3 after the anodization process and calcination at 450 °C, resulting in the formation of the rutile phase. **Figure 1b** shows samples 1 and 2 also subjected to anodization using the same procedure as sample 3 and calcined at 350 °C; sample 1 was calcined for 5 hours and sample 2 for 2 hours. This anodization process is crucial to form an oxide layer that facilitates the attainment of the desired phases without the need for prolonged times or high calcination temperatures, unlike literature reports (Çomaklı, 2015; Jianguo, 2010) suggesting temperatures of 500-700 °C for the anatase phase and 900 °C for the rutile phase. This underscores the significant role of anodization prior to calcination in achieving the desired phases. **Figure 1** also reveals a broad peak at approximately 15°, 2θ, corresponding to titanium (Ti), attributed to the formation of a very

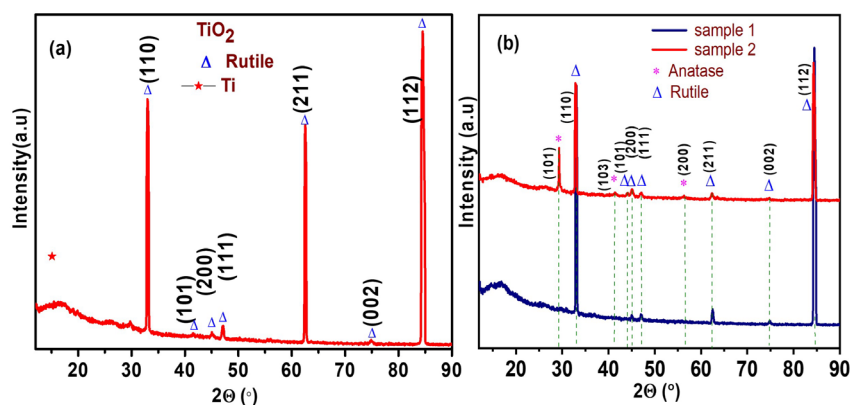


Figure 1. XRD patterns: **a.** Sample 3, calcined at 450 °C for two hours. **b** Samples 1 and 2 calcined at 350 °C for two hours (sample 2) and five hours (sample 1)

thin layer of titanium oxide during the anodization process on the foil leaving the titanium visible beneath this oxide layer. The calcination process of the samples and the duration of this process play a crucial role in the formation of the rutile and anatase phases.

Figure 1 illustrates the three samples post-anodization and calcination at varying temperatures. Rutile, characterized by a tetragonal structure with six atoms per unit cell, emerges as the most stable, featuring a slight orthorhombic distortion in the TiO_6 octahedron. Within the rutile unit cell, four oxygen atoms create a partial octahedron around Ti, while two titanium atoms (at positions $[0, 0, 0]$ and $[1/2, 1/2, 1/2]$) are individually positioned (Reference code: 01-088-1175) (Kim, 2021). Conversely, the distortion of the TiO_6 octahedron is notably more pronounced in the anatase phase that possesses a tetragonal structure (Kim, 2021; Gonçalves, 2018). Consequently, the symmetry of anatase is inferior to orthorhombic. The anatase unit cells comprise four titanium atoms at $[1/2, 1/2, 1/2]$, $[0, 0, 0]$, $[1/4, 0, -1/4]$, and $[0, 1/2, 1/4]$, and eight oxygen atoms shaping a partial TiO_6 octahedron around Ti, with each octahedron edge divided into four (Reference code: 96-101-0943).

Rutile arranges into a linear chain, whereas anatase adopts zigzag chains with a helical axis where each octahedron connects to eight other octahedra (four through shared edges and four through corners). Compared to rutile, Ti-Ti distances in anatase are larger and Ti-O distances are smaller. A slight orthorhombic distortion is observed in rutile, more pronounced in anatase. These structural disparities yield different densities and electronic band configurations. At elevated temperatures, phase transformations occur, occasionally converting anatase into rutile. Under certain experimental conditions such as high-energy milling operations, anatase may transform into amorphous phases rather than rutile. At macro and microscopic scales, rutile is deemed the thermodynamically stable phase under ambient conditions, despite anatase crystallizing first (Gonçalves, 2018). Here, we obtained the rutile phase through an anodization process followed by rapid high-temperature calcination.

In TiO_2 photocatalysis applications, the significance of the structure, whether in the form of rutile or anatase, lies in its direct influence on the photocatalytic activity of the material. This activity is affected by various factors: phase structure, crystallite size, specific surface area, and pore structure, among others. Although rutile has a smaller energy gap than anatase, its photocatalytic activity is lower due to faster electron and hole recombination rates, larger grain size, and smaller specific surface area (Ali, 2018). These findings suggest that both the crystalline structure and the physical properties of TiO_2 play a crucial role in its ability to catalyze photocatalytic reactions with significant implications for applications such as the decomposition of organic pollutants in the environment and solar energy generation. **Table 1** summarizes the phases we identified, namely rutile and anatase, and their characteristics.

The sample in **figure 1a** exhibits a rutile structure after undergoing anodization and calcination at 450 °C. Conversely, **figure 1b** shows the coexistence of both anatase and rutile phases alongside titanium. These findings underscore how minor adjustments in the anodization process or calcination temperature can significantly impact the structural phase of the samples.

Table 1. Comparing the crystal structures of TiO_2 nanostructures

Properties	Rutile	Anatase
Crystal structure	Tetragonal	Tetragonal
Space group	P42/mnm	I41/amd
Lattice constant (Å)	$a, b = 4.5170$ $c = 2.9400$	$a, b = 3.7300$ $c = 9.3700$
Density (g cm^{-3})	4.42	4.07
Volume/molecule (Å ³)	31.21	34.061 (Ali, 2018)

According to roughness parameters, the coating of the structure that grew after anodizing on the titanium surface generally exhibits a regular and homogeneous surface (**Figure 2a**) and a tubular structure with some presence of voids or removal of peaks. **Figure 2b** shows more voids and the sample is less homogeneous. In other words, examining the surface profiles reveals that sample 1 exhibits a relatively smooth surface (**Figure 1a**), whereas sample 3 appears much rougher with several defects visible. Several researchers have noted that increased surface roughness typically leads to higher surface hydrophilicity (**Zhou, 2019**).

The main parameter calculated from the Tafel polarization curves in **figure 3** was the corrosion rate of the anodic samples on the titanium substrate. Sample 1 exhibited the lowest corrosion rate and sample 2 the highest. Additionally, the most negative E_{corr} value corresponded to sample 1 and the least negative to sample 3 (**Table 2**). These electrochemical test results suggest that sample 1 has better anticorrosive properties and sample 2 exhibits greater deterioration and less corrosion resistance (**Camargo, 2009**).

Figure 3 illustrates Tafel potentiodynamic curves with the rutile curve displaying the lowest corrosion density among the samples. This suggests structural changes following calcination likely influenced by mechanical and thermal factors. These alterations are reflected in **table 2** where sample 2 exhibits superior corrosion resistance indicating a significant increase in corrosion density and velocity likely induced by microstructural variations due to applied voltages (**Lee, 2020; Li, 2019; Luttrell, 2014**).

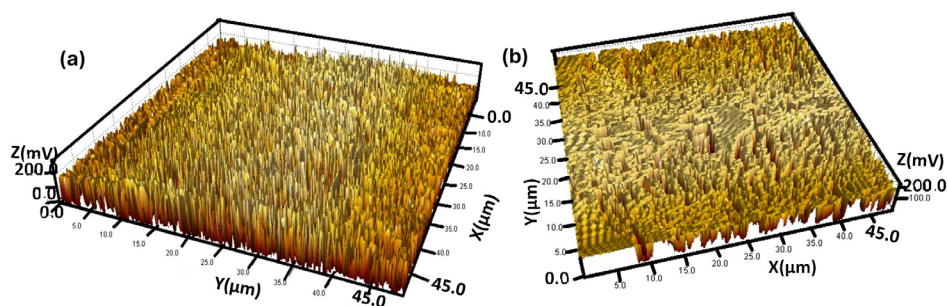


Figure 2. Atomic force microscopy (AFM) images of sample 1 calcined at 350 °C and sample 3 calcined at 450 °C for two hours

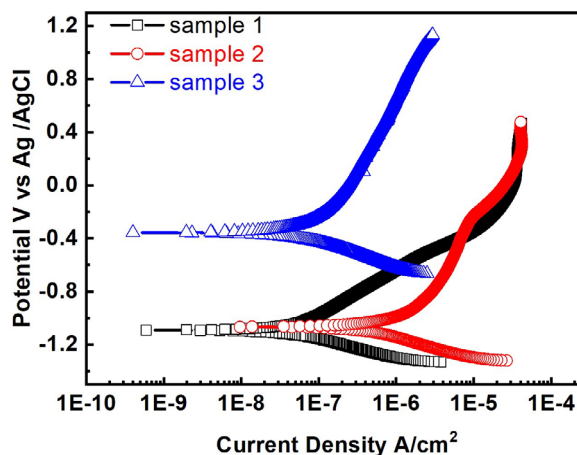
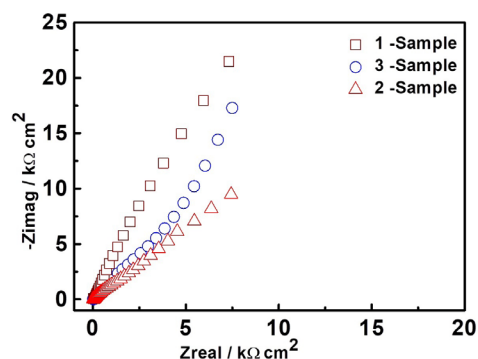


Figure 3. Tafel potentiodynamic curves of the anodized titanium samples obtained through the friction-stir agitation process

Table 2. Corrosion rate in the samples

	Sample 1	Sample 2	Sample 3
I _{corr}	52.80 nA /cm ²	1750 nA/cm ²	105.0 nA/cm ²
E _{corr}	-1.09 V vs Ag/AgCl	-1.07 V vs Ag/AgCl	-0.356 V vs Ag/AgCl
Corrosion R _a mpy	72.42 e ⁻³	2.403	144.1 e ⁻³
Chi Squared	1.61	4.9	1.8 e ⁻¹

**Figure 4.** Coating impedance data

A notable correlation emerges between the initial corrosion potential recorded in each EIS measurement and the estimated values obtained from EIS data adjustments (as listed in **table 2**). This correlation highlights an increase in E_{corr} associated with a reduction in the surface area occupied by anodic regions and the expansion of oxide-protected areas.

Potentiodynamic polarization curves in **figure 3** provide valuable insights into surface changes. **Figure 4** complements this with electrochemical impedance spectroscopy (EIS) of charge transfer and recombination processes at the photoelectrode-electrolyte interfaces (**Monetta**, 2017). EIS facilitates the comparison of structural properties and corrosion resistance among samples with different TiO_2 crystalline phases (rutile and anatase) correlating directly with the results of electrochemical tests. It also reveals how variations in the process such as calcination times, calcination temperature, or the composition of the anodizing electrolyte affect the structural properties and corrosion resistance of TiO_2 coatings. Parte superior do formulário

Conclusions

Our results underscore the pivotal role of calcination parameters, specifically temperature and time, in shaping the phase composition and corrosion resistance of anodized TiO_2 coatings. By systematically varying the calcination conditions post-anodization, we successfully synthesized both rutile and anatase phases of titanium dioxide. Our findings highlight that even minor adjustments in the calcination process significantly influence the observed structural phases. Furthermore, our electrochemical analyses, including Tafel polarization curves and impedance spectroscopy, provided valuable insights into the corrosion behavior of these coatings. Samples subjected to longer calcination durations exhibited lower corrosion rates, indicative of enhanced corrosion resistance. This correlation emphasizes the critical importance of optimizing calcination parameters to achieve desired crystalline phases and enhance material properties such as corrosion resistance. These results suggest promising applications in biocompatible coatings and environments prone to mechanical wear and corrosive conditions.

Acknowledgments

We thank Professor Jorge Bautista at the Francisco de Paula Santander University in Cúcuta for facilitating the laboratory space for sample collection, and to the Universidad Nacional de Colombia and the Universidad Militar Nueva Granada.

Author contributions

M.R. Joya contributed to sample acquisition and manuscript drafting. W. A. did the experimental measurements and revisions. J.B.O. oversaw the revision and discussion.

Conflicts of interest

The authors declare that there is no conflict of interests of any kind regarding the publication of the results of our research work.

References

- Ali, I., Suhail, M., Alothman, Z. A., Alwarthan, A. (2018). Recent advances in syntheses, properties and applications of TiO₂ nanostructures. *RSC Advances*, 8(53), 30125-30147. <https://doi.org/10.1039/c8ra06517a>
- Aperador, W., Ramírez, C., Caicedo, J.C. (2012). The effect of Ti(CN)/TiNb(CN) coating on erosion-corrosion resistance. *Ingeniería e investigación*, 32(2), 6-11. <https://doi.org/10.15446/ing.investig.v32n2.37522>
- Arzaee, N. A., Yodsin, N., Ullah, H., Sultana, S., Mohamad N. M. F., Mahmood Zuhdi, A. W., Mohd Yusoff, A. R. B., Jungstuttiwong, S., Mat Teridi, M. A. (2023). Enhanced hydrogen evolution reaction performance of anatase-rutile TiO₂ heterojunction via charge transfer from rutile to anatase. *Catalysis Science & Technology*, 13(24), 6937-6950. <https://doi.org/10.1039/D3CY00918A>
- Baram, N. & Ein-Eli, Y. (2010). Electrochemical Impedance Spectroscopy of Porous TiO₂ for Photocatalytic Applications. *The Journal of Physical Chemistry C*, 114(21), 9781-9790. <https://doi.org/10.1021/jp911687w>
- Bautista-Ruiz, J. H., Raba, A. M., Joya, M. R. (2018). Influence of the H₂O content and the time on the formation of nanostructures in a chemical solution of H₂O/HF/NH₄F/EG. *Journal of Physics: Conference Series*, 1126(1), 012042. <https://doi.org/10.1088/1742-6596/1126/1/012042>
- Camargo, A., Aperador C., W. A., Ríos, A., Ortiz, C., Vera, E. (2009). Caracterización mediante espectroscopía de impedancia electroquímica de películas anódicas crecidas sobre Al 2024-T3. *Revista de la Sociedad Colombiana de Física*, 41(2), 261-263.
- Çomaklı, O., Yazıcı, M., Yetim, T., Yetim, A.F., Çelik, A. (2015). The effect of calcination temperatures on structural and electrochemical properties of TiO₂ film deposited on commercial pure titanium. *Surface and Coatings Technology*, 285, 298-303. <https://doi.org/10.1016/j.surfcoat.2015.11.055>
- Eddy, D.R., Permana, M.D., Sakti, L.K., Sheha, G.A.N., Solihudin; Hidayat, S., Takei, T., Kumada, N., Rahayu, I. (2023). Heterophase Polymorph of TiO₂ (Anatase, Rutile, Brookite, TiO₂ (B)) for Efficient Photocatalyst: Fabrication and Activity. *Nanomaterials*, 13, 704. <https://doi.org/10.3390/nano13040704>
- Gabellini, L., Calisi, N., Martinuzzi, S. M., Taurino, R., Innocenti, M., Bacci, T., Borgioli, F., Galvanetto, E., Caporali, S. (2023). Effect of Bath Composition on Titanium Anodization Using the Constant-Current Approach: A Crystallographic and Morphological Study. *Coatings*, 13(7), 1284. <https://doi.org/10.3390/coatings13071284>
- Gonçalves, M., Pereira, J., Matos, J., Vasconcelos, H. (2018). Photonic Band Gap and Bactericide Performance of Amorphous Sol-Gel Titania: An Alternative to Crystalline TiO₂. *Molecules*, 23(7), 1677. <https://doi.org/10.3390/molecules23071677>
- Jiaguo Y. & Bo W. (2010). Effect of calcination temperature on morphology and photoelectrochemical properties of anodized titanium dioxide nanotube arrays. *Applied Catalysis B: Environmental*, 94(3-4), 295-302. <https://doi.org/10.1016/j.apcatb.2009.12.003>
- Kim, M. G., Kang, J. M., Lee, J. E., Kim, K. S., Kim, K. H., Cho, M., Lee, S. G. (2021). Effects of Calcination Temperature on the Phase Composition, Photocatalytic Degradation, and Virucidal Activities of TiO₂ Nanoparticles. *ACS Omega*, 6(16), 10668-10678. <https://doi.org/10.1021/acsomega.1c01684>
- Kim, S. A., Hussain, S. K. K., Abbas, M. A., Bang, J. H. (2022). High-temperature solid-state rutile-to-anatase phase transformation in TiO₂. *Journal of Solid-State Chemistry*, 315, 123510. <https://doi.org/10.1016/j.jssc.2022.123510>

- Lee, V. S., Cho, A. Y., Rim, Y. S., Park, J.-Y., Choi, T. (2020). Synergistic Design of Anatase–Rutile TiO₂ Nanostructured Heterophase Junctions toward Efficient Photoelectrochemical Water Oxidation. *Coatings*, 10(6), 557. <https://doi.org/10.3390/coatings10060557>
- Li, B., Zhang, L., Li, Y., Li, H., Zhou, L., Liang, C., Wang, H. (2019). Corrosion resistance and biological properties of anatase and rutile coatings on titanium surface. *Chemistry Letters*, 48, 1355-1357. <https://doi.org/10.1246/cl.190549>
- Li, L., Lyu, L., Gui, J., Sun, X., Qian, Y., Yang, G. (2019). Facet-dependent interfacial charge transfer in TiO₂/nitrogen-doped graphene quantum dots heterojunctions for visible-light driven photocatalysis. *Catalysts*, 9(4), 345. <https://doi.org/10.3390/catal9040345>
- Lin, J., Heo, Y. U., Nattestad, A., Bachmatiuk, A., Ha, J. S., Zhang, X. (2014). 3D hierarchical rutile TiO₂ and metal-free organic sensitizer producing dye-sensitized solar cells with 8.6% conversion efficiency. *Scientific Reports*, 4, 5769. <https://doi.org/10.1038/srep05769>
- Luttrell, T., Halpegamage, S., Tao, J., Kramer, A., Sutter, E., Batzill, M. (2014). Why is anatase a better photocatalyst than rutile - Model studies on epitaxial TiO₂ films. *Scientific Reports*, 4, 4043. <https://doi.org/10.1038/srep04043>
- Manut, A.S., Zoolfakar, M.H. Mamat, N.S., Ghani, Ab M. Zolkapli, M. (2020) Characterization of Titanium Dioxide (TiO₂) Nanotubes for Resistive-type Humidity Sensor. *IEEE International Conference on Semiconductor Electronics (ICSE)*, Kuala Lumpur, Malaysia, 2020, pp. 104-107, <https://doi.org/10.1109/ICSE49846.2020.9166854>
- Mansfeldova, V., Mansfeldova, V., Zlamalova, M., Tarabkova, H., Janda, P., Vorokhta, M., Piliat, L., Kavan, L. (2021). Work Function of TiO₂ (Anatase, Rutile, and Brookite) Single Crystals: Effects of the Environment. *The Journal of Physical Chemistry C*, 125(3), 1902-1912. <https://doi.org/10.1021/acs.jpcc.0c10519>
- Mateus, H. M., Bautista-Ruiz, J., Barba-Ortega, J., Joya, M. R. (2019). Formation of titanium oxide nanotube arrays by controlling H₂O and time through anodic oxidation. *Rasyan. Journal of Chemistry*, 12(3), 1304-1314. <https://doi.org/10.31788/RJC.2019.1235265>
- Monetta, T., Acquesta, A., Carangelo, A., Bellucci, F. (2017). TiO₂ nanotubes on Ti dental implant. Part 2: EIS characterization in Hank's solution. *Metals*, 7(6), 220. <https://doi.org/10.3390/met7060220>
- Parambil, N. S. K., Raphael, S. J., Joseph, P., Dasan, A. (2023). Recent advancements toward visible-light-driven titania-based nanocomposite systems for environmental applications: An overview. *Applied Surface Science Advances*, 18, 100487. <https://doi.org/10.1016/j.apsadv.2023.100487>
- Pasquale, L., Tavella, F., Longo, V., Favaro, M., Perathoner, S., Centi, G., Ampelli, C., Genovese, C. (2023). The Role of Substrate Surface Geometry in the PhotoElectrochemical Behavior of Supported TiO₂ Nanotube Arrays: A Study Using Electrochemical Impedance Spectroscopy (EIS). *Molecules*, 28, 3378. <https://doi.org/10.3390/molecules28083378>
- Quitério, P., Apolinário, A., Sousa, C. T., Costa, J. D., Ventura, J., Araújo, J. P. (2015). The cyclic nature of porosity in anodic TiO₂ nanotube arrays. *Journal of Materials Chemistry A*, 3(7), 3692-3698. <https://doi.org/10.1039/c4ta04607b>
- Sarngan, P. P., Lakshmanan, A., Sarkar, D. (2022). Influence of Anatase-Rutile Ratio on Band Edge Position and Defect States of TiO₂ Homo Junction *Catalyst*. *Chemosphere*, 286 (Part 2), 131692. <https://doi.org/10.1016/j.chemosphere.2021.131692>
- Sanoja-López, K. A., Loo-Molina, N. S., Luque, R. (2024). An overview of photocatalyst eco-design and development for green hydrogen production. *Catalysis Communications*, 106859. <https://doi.org/10.1016/j.catcom.2024.106859>
- Suhadolnik, L., Marinko, Ž., Ponikvar-Svet, M., Tavčar, G., Kovač, J., & Čeh, M. (2020). Influence of Anodization-Electrolyte Aging on the Photocatalytic Activity of TiO₂ Nanotube Arrays. *Journal of Physical Chemistry C*, 124(7), 4073-4080. <https://doi.org/10.1021/acs.jpcc.9b09522>
- Thakur, N., Thakur, N., Kumar, A., Thakur, V. K., Kalia, S., Arya, V., Kumar, A., Kumar, S., Kyzas, G. Z. (2024). A critical review on the recent trends of photocatalytic, antibacterial, antioxidant and nanohybrid applications of anatase and rutile TiO₂ nanoparticles. *Science of The Total Environment*, 914, 169815. <https://doi.org/10.1016/j.scitotenv.2023.169815>
- Yu, H., Li, S., Peng, S., Yu, Z., Chen, F., Liu, X., Guo, J., Zhu, B., Huang, W., Zhang, S. (2023). Construction of rutile/anatase TiO₂ homo junction and metal-support interaction in Au/TiO₂ for visible photocatalytic water splitting and degradation of methylene blue. *International Journal of Hydrogen Energy*, 48(3), 975-990. <https://doi.org/10.1016/j.ijhydene.2022.10.010>
- Zhou, L., Liang, C., Wang, H. (2019). Corrosion resistance and biological properties of anatase and rutile coatings on titanium surface. *Chemistry Letters*, 48, 1355-1357. <https://doi.org/10.1246/cl.190549>